Mem. S.A.It. Vol. 79, 579

Memorie della

Impact of rotation on the evolution of low–mass stars

D. Brown[1], M. Salaris[1], S. Cassisi[2], and A. Pietrinferni[2]

[1] Astrophysics Research Institute – Liverpool John Moores University, Twelve Quays House, Egerton Wharf, Birkenhead, CH41 1LD, United Kingdom
e-mail: db@astro.livjm.ac.uk
[2] Instituto Nazionale di Astrofisica, Osservatorio Astronomico di Collurania "Vincenzo Cerulli", Via Mentore Maggini s.n.c., 64100 Teramo, Italy

Abstract. High precision photometry and spectroscopy of low–mass stars reveal a variety of properties standard stellar evolution cannot predict. Rotation, an essential ingredient of stellar evolution, is a step towards resolving the discrepancy between model predictions and observations.
The first rotating stellar model, continuously tracing a low–mass star from the pre–main sequence onto the horizontal branch, is presented. The predicted luminosity functions of stars of globular clusters and surface rotation velocities on the horizontal branch are discussed.

Key words. Stars: Rotation – Stars: Population II – Stars: Horizontal Branch – Galaxy: globular clusters

1. Introduction

Rotation has to be included in realistic stellar models. Since recent high precision photometry and spectroscopy have become available, the effects of slower rotation on low–mass stars has become detectable in the colour–magnitude diagram (CMD) and Luminosity Functions (LFs). To predict them precisely, low–mass stellar models need to take rotation into account.

1.1. Stellar structure

The version of the stellar evolution code FRANEC, described in Pietrinferni et al. (2004), is used for our computations. Rotation was included in the stellar structure equations following the prescription of Kippenhahn & Thomas (1970). The required parameters f_P and f_T were derived analytically from the effective gravitational potential of the star approximating its equipotential surfaces as rotational ellipsoids.

We have eliminated the subatmospheric region used in the original code and increased the density of the outermost meshpoints in the stellar model.

1.2. Transport mechanisms

Chemical elements and angular momentum are transported within the star during its evolution. In a convective zone (CZ) the transport is assumed to be instantaneous. The

Send offprint requests to: D. Brown

abundance of chemical elements is averaged in a CZ and the angular momentum redistributed to achieve either specific angular momentum conservation or solid body rotation. Both distributions are limiting cases introduced by Sweigart & Mengel (1979). Solid body rotation is chosen for CZ until the the star reaches the turn off (TO), after which the specific angular momentum is conserved (see Palacios & Brun 2006 and Sills & Pinsonneault 2000).

In a radiative region the transport is a diffusive process, since Palacios et al. (2006) have shown that advective transport via meridional currents is less efficient than via diffusion resulting from the shear instability. This instability dominates rotational mixing (Zahn 1992). The diffusion coefficient D_v is taken from Denissenkov & Weiss (2004) introducing an efficiency parameter F. Chemical elements are transported by a combination of atomic diffusion and rotational mixing. Angular momentum is diffused by rotational mixing alone.

1.3. Braking

The total amount of angular momentum of the star is changed by several processes. On the pre-main sequence (PMS) magnetic fields connect the star with its circumstellar disk. The disk allows angular momentum to be diffused beyond the influence of the magnetic field of the star, preventing the PMS spin-up. This process of disk braking (Shu et al. 1994) is active until a time $\tau_{\rm DB}$.

On the main sequence (MS) the stellar magnetic field increases the amount of angular momentum lost by its stellar wind. The angular momentum lost by this magnetic–wind braking is given by Chaboyer, Demarque, & Pinsonneault (1995). We include a function determining the efficiency to generate a magnetic field $B_{\rm eff}$ and parametrise it by the mass of the convective envelope. The shape of $B_{\rm eff}$ is determined by two parameters (M_w;B_w). The overall efficiency of the braking process is determined by f_k.

Angular momentum lost via mass loss is already included in the code, and is dominant on the red giant branch (RGB).

2. Calibration

The modified stellar evolution code contains a number of free parameters. First, the two parameters describing the initial conditions of the star have to be determined: the initial rotation rate ω_0 and the disk braking time τ_B. Four additional parameters to be calibrated are: the mixing length α, the braking efficiency $f_{\rm k}$, the function describing the efficiency to generate the magnetic field $B_{\rm eff}$, and the rotational mixing efficiency F.

2.1. Initial conditions

To determine ω_0 we used the rotation period of a sample of ∼1 Myr old stars from three open cluster: IC 348 (Littlefair et al. 2005), Orion Nebula Cluster (Herbst et al. 2002), and the Orion Nebula Cluster Flanking fields (Rebull 2001). We limited the mass range to $0.5\,M_\odot < M < 1.3\,M_\odot$ to later reproduce the surface rotation velocity for the Hyades. The mean value of the rotation period at 1 Myr is $P_{1\,\rm Myr} = (5\pm4)$ d. Appropriate values of ω_0 for our stellar models were chosen to reproduce $P_{1\,\rm Myr}$. This ω_0 is derived from stars with solar metallicity. To determine ω_0 at lower metallicites, the total angular momentum of stars of the same mass, but different metallicity, is assumed to be the same at the start of their life on the PMS.

The disk braking time is set to $\tau_{\rm DB} = 5$ Myr, at which 50 % of the stars in clusters have no longer a circumstellar disk (Bouvier, Forestini, & Allain 1997).

2.2. Free parameters

To calibrate the mixing length (α) and f_k we created a theoretical solar model. The predicted rate of angular momentum loss $\left(\frac{{\rm d}J}{{\rm d}t}\right)$ for the model was used to confirm the adopted braking mechanisms. In Fig. 1 we give the rate of angular momentum loss for three different solar models with initial rotation rates consistent with observed $P_{1\,\rm Myr}$ ($P_{1\,\rm Myr}$=5 d grey line, $P_{1\,\rm Myr}$=12 d thick light grey line, and $P_{1\,\rm Myr}$=1 d thin black line). Each of these models reaches $\left(\frac{{\rm d}J}{{\rm d}t}\right)$ observed for the Sun and

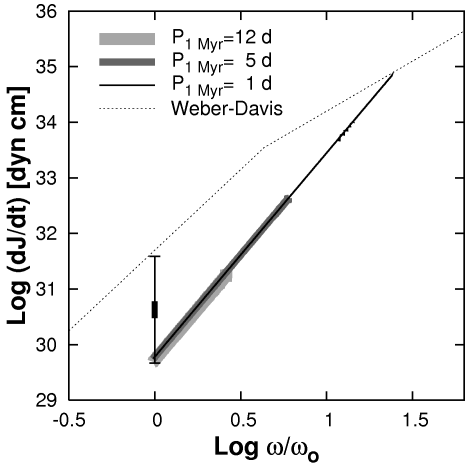

Fig. 1. Rate of angular momentum loss ($\frac{dJ}{dt}$) by magnetic wind braking plotted against surface rotation rate of three different solar models ($P_{1\,\mathrm{Myr}}$=5 d grey line, $P_{1\,\mathrm{Myr}}$=12 d thick light grey line, and $P_{1\,\mathrm{Myr}}$=1 d thin black line). Observed $\frac{dJ}{dt}$ values for the Sun (log $\frac{\omega}{\omega_0}$=0) and a theoretically derived upper limit (dotted line) for the MS is shown (see text for details).

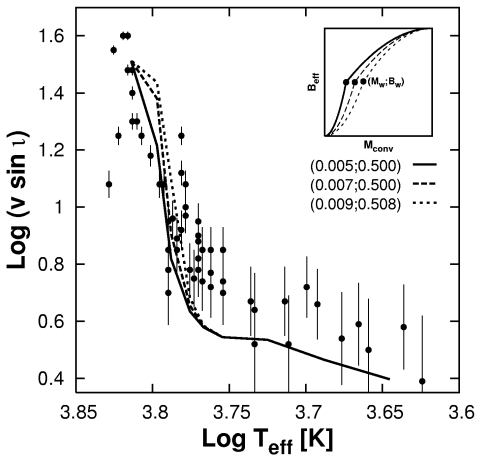

Fig. 2. The observed $\langle v \sin \iota \rangle$ taken from Soderblom et al. (1993) as a function of T_{eff}. The profile of the B_{eff} functions are given in the inset to the upper right, including the point (M_{w};B_{w}) that defines its shape. Isochrones for $\langle v \sin \iota \rangle$ are shown using different B_{eff} functions: (0.005;0.500) solid, (0.007;0.500) long dashed, and (0.009;0.508) short–dashed line.

shown in Fig. 1. Additionally, they lie below a theoretical upper limit determined by a 2D Weber & Davis (1967) equatorial wind model.

B_{eff} was determined by predicting surface rotation velocities for the Hyades and comparing them with observations by Soderblom et al. (1993). Figure 2 shows three predicted rotation distributions for different choices of the B_{eff} function ((0.005;0.500) solid, (0.007;0.500) long dashed, and (0.009;0.508) short–dashed line). The profile of the B_{eff} functions are given in the inset to the upper right, including the point (M_{w};B_{w}) that defines its shape. The best fit between data and models was reached with (0.005;0.500).

Spectroscopic observations that in the past were explained in terms of efficient rotational mixing are now being challenged by new data and theoretical developments (see Spite plateau data of Asplund et al. 2006 presented in Bonifacio et al. 2007; Eggleton, Dearborn, & Lattanzio (2007), P. Ventura and E. Carretta in this proceedings, for the issue of extra mixing on the RGB). Therefore, the rotational mixing efficiency F is set to an arbitrary low value of 10^{-6}, allowing for a marginal transport without creating any significant changes to the chemical abundances in the stellar model.

3. Application to GC

Using our rotating stellar models we present a comprehensive analysis of rotational effects on the evolution of low–mass stars in globular clusters. Past work was exploratory (Vandenberg, Larson, & De Propris 1998) or targeted specific issues (Palacios et al. 2006). We apply our models to typical globular cluster stars (Z=10^{-3} and Y=0.246) and corresponding isochrones of 10.5 and 12.0 Gyr.

3.1. Surface velocities

Our isochrones predict a surface velocities on the SGB $v_{\mathrm{surf}} = 1 - 5.5\,\mathrm{km\,s^{-1}}$, consis-

tent with the observed $v_{\rm surf} \sim 3\,{\rm km\,s^{-1}}$ by Lucatello & Gratton (2003). More precise observations of the rotation along the SGB are necessary to further constrain the initial conditions and the angular momentum transport in CZs.

Rotational velocities on the HB were determined for a $0.8\,{\rm M}_{\odot}$ star experiencing no mass loss with an optimised version of our rotational code that is able to evolve through the helium flash. We predicted $v_{\rm surf}$ = $6.85\,{\rm km\,s^{-1}}$ on the zero–age HB (ZAHB) that is within the range observed for red HB stars (Sills & Pinsonneault 2000).

3.2. Isochrones

Two isochrones for ages of 10.5 and 12.0 Gyr are shown in Fig. 3, with (dashed line) and without rotation (solid line). Rotation does not shift the MS or the TO, however, the brightness of the SGB at (B-V)=0.55 is slightly increased by 0.05 and 0.03 mag, for 10.5 and 12.0 Gyr respectively. The RGB at $M_V = 2$ including rotation is bluer by 0.01 and 0.007 mag for 10.5 and 12.0 Gyr respectively.

Rotation increases the tip of the RGB (TRGB) luminosity by $\Delta \log L/L_{\odot} = 0.08$ and the helium core mass at the flash by $\Delta M_{\rm He} = 0.048\,M_{\odot}$. This large helium core leads to a brighter ZAHB luminosity of $\Delta M_V = 0.326$ when including rotation, and will be discussed later.

3.3. Luminosity functions

From the isochrones we then determine the LF for the case of rotation and no rotation using a Salpeter (1955) initial mass function. Figure 4 shows the two cases are normalised at a M_V=4 which is close to the TO and independent of the choice of initial mass function. The shape of the RGB bump is not changed by rotation, only its location is shifted to brighter luminosities by $\Delta M_V = 0.1$ for the 10.5 Gyr LF. Similar to Vandenberg, Larson, & De Propris (1998), we find that rotation reduces the SGB slope and increases the number count at the base of the RGB (by 11 % for the 12 Gyr LF).

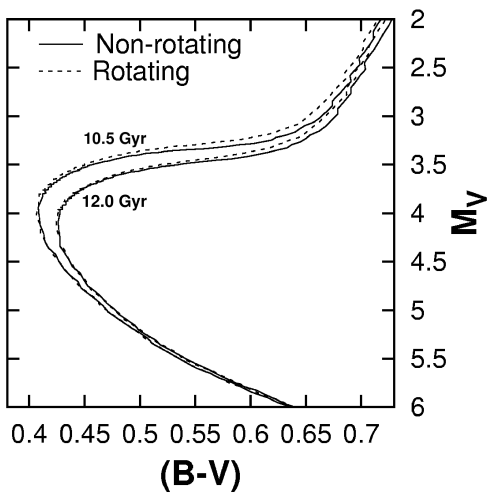

Fig. 3. The 10.5 Gyr and 12 Gyr isochrones without rotation (as labelled) are plotted in a BV CMD as solid lines. The isochrones including rotation are shown as dashed lines.

4. Discussion

Given an isochrone without rotation that is consistent with observational constraints. The inclusion of rotation increases the helium core mass, this leads to a brighter ZAHB and distances from HB fitting that are no longer consistent with parallax based empirical MS fitting (Recio–Blanco et al. 2004).

A solution would be to reduce the rotation rate in the helium core on the RGB. This reduction may result from either more realistic angular momentum transport in CZs (see exploratory work by Palacios & Brun 2006) or reducing ω_0.

We chose to reduce the initial rotation rate by adopting a different method to transpose solar metallicity rotation rates to lower metallicities. Instead of keeping the total amount of initial angular momentum constant, ω_0 is defined so that these stars reach a rotational period of $P_{1\,\rm Myr}$=5 d. This reduces ω_0 by 60 % and leads to a SGB rotation velocity of $3\,{\rm km\,s^{-1}}$, consistent with observations. The ZAHB including rotation is only brighter by ΔM_V=0.122 (comparable to typical photometric errors for HB stars) and leads to ages younger by 1.5 Gyr.

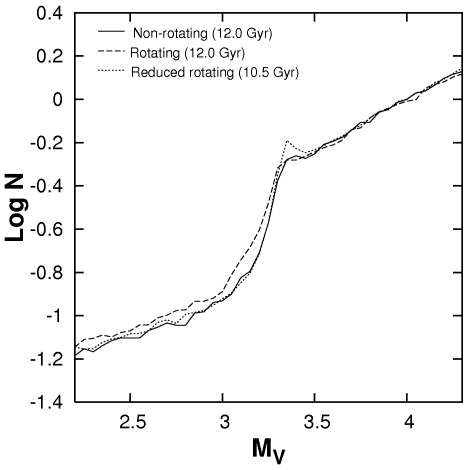

Fig. 4. Three LFs are shown as a function of M_V with an age of 12 Gyr without (solid line) and with rotation (dashed lines), as well as an age of 10.5 Gyr including the reduced initial rotation (dotted line).

Therefore, an isochrone or LF with and without rotation can only be consistent with observational constraints, if the rotational isochrone or LF is 1.5 Gyr younger than without rotation.

A consistent comparison between a 10.5 Gyr old LF with the reduced ω_0 (solid line) and a 12.0 Gyr LF without (dashed line), is shown in Fig. 4. The prior determined 11 % increase in number count is reduced to 5 %, but it is still detectable.

Acknowledgements. I am grateful to S. Cassisi and A. Pietrinferni for enabling several research stays at Teramo observatory for me and the valuable discussions furthering the understanding of FRANEC and the helium flash code. Furthermore, I would like to acknowledge the RAS for their financial support.

References

Asplund, M., et al. 2006, ApJ, 644, 229
Bonifacio, P., et al. 2007, A&A, 462, 851
Bouvier, J., Forestini, M., & Allain, S. 1997, A&A, 326, 1023
Chaboyer, B., Demarque, P., & Pinsonneault, M. H. 1995, ApJ, 441, 865
Denissenkov, P. A., & Weiss, A. 2004, ApJ, 603, 119
Eggleton, P. P., Dearborn, D. S. P., & Lattanzio, J. C. 2004, ArXiv Astrophysics e-prints, 0706.2710
Herbst, W., et al. 2002, A&A, 396, 513
Kippenhahn, R., & Thomas, H. C. 2002, 'Stellar Rotation', A. Slettebak
Littlefair, S. P., et al. 2005, MNRAS, 358, 341
Lucatello, S., & Gratton, R. G. 2003, A&A, 406, 691
Palacios, A., & Brun, A. S. 2006, ArXiv Astrophysics e-prints, 0610040
Palacios, A., et al. 2006, A&A, 453, 261
Pietrinferni, A., et al. 2004, ApJ, 612, 168
Rebull, L. M. 2001, AJ, 121, 1676
Recio–Blanco, et al. 2001,A&A, 417,597
Salpeter, E. E. 1955, ApJ, 161,161
Shu, F., et al. 1994, AJ, 429, 781
Sills, A., & Pinsonneault, M. H. 2000, ApJ, 540, 489
Soderblom, D. R., et al. 1993, ApJ, 409, 424
Sweigart, A. V., & Mengel, J. G. 1979, ApJ, 229, 624
Vandenberg, D. A., Larson, A. M., & De Propris, R. 1998, PASP, 110, 98
Weber, E. J., & Davis, L. 1967, ApJ, 148, 217
Zahn, J.–P. 1992, A&A, 265, 115